Modeling of Carbon Dioxide Absorption by Solution of Piperazine and Methyldiethanolamine in a Rotating Packed Bed

Arash Esmaeili [a], Amin Tamuzi [b], Tohid N. Borhani [c], Yang Xiang [a], Lei Shao [a*]

[a] Research Center of the Ministry of Education for High Gravity Engineering and Technology, Beijing University of Chemical Technology, Beijing 100029, China.

[b] Computer Aided Process Engineering (CAPE) Laboratory, School of Chemical, Petroleum and Gas Engineering, University of Science and Technology, Tehran 1684613114, Iran

[c] Faculty of Science and Engineering, University of Wolverhampton, Wolverhampton WV1 1LY, The United Kingdom

* Corresponding author

Email Address: shaol@mail.buct.edu.cn

Tel.: +86 10 64421706, +86 136 4109 2152

Abstract

CO_2 removal by the blended amine solution of piperazine (PZ) and methyldiethanolamine (MDEA) with the various molar concentration ratios in a rotating packed bed (RPB) was modelled using MATLAB linked to Aspen Plus. All the required correlations for the RPB in addition to the mass and energy balances were written in MATLAB while the demanded physical and transport properties were extracted from Aspen Plus. The similar operating conditions and compositions in the reported experiments were used to run the model by the two-film theory for mass transfer as steady state, while the impact of five different parameters on the CO_2 absorption efficiency was examined to validate the model. The modeling results are in good agreement with the experimental data for which the average absolute deviation is less than 7.0%. The process analysis revealed that rotational speed and PZ concentration have the most significant effects on CO_2 absorption efficiency.

Keywords: Absorption, Aspen Plus, Carbon dioxide, MATLAB, Piperazine, Rotating Packed Bed

1. Introduction

The CO_2 emission has led to the global warming and the greenhouse effect in the recent century and has raised extreme concerns related to the environmental issues and international economics. Among the greenhouse gases, the contribution of CO_2 to the increase of the atmospheric temperature accounts for more than 60% [1]. It has been reported that CO_2 concentration in the atmosphere has increased by about 40% in comparison with that in the pre-industrial times, and exceeded 400 ppm which is higher than pre-industrial level of about 300 ppm due to fossil fuel combustion as the primary reason of CO_2 emission [2]. One of those fossil fuels is coal which is widely used in a great number of power plants [3]. It should be noted that such power plants will be a main source for the generation of energy and power in the next few decades due to the increase in the world population and demands of economic growth. Therefore, it is vital to reduce CO_2 emission by developing reliable, safe and viable technologies to tackle the huge challenge of global warming.

A variety of technologies and processes have been developed to mitigate CO_2 emissions, such as absorption, adsorption, membrane separation, terrestrial sequestration and chemical looping combustion [4]. The chemical absorption of CO_2 using different amine solutions has been broadly studied by many researchers using the conventional columns such as packed towers, spray columns and bubble columns with CO_2 removal efficiencies reaching 55-95% [5]. It has been proved that the chemical CO_2 absorption is one of the most mature processes around the world to remove this greenhouse gas; however, it must be mentioned that the size reduction of the vertical columns is difficult due to mass transfer limitations, and there are still major obstacles for improving the performance of the conventional columns. The main barriers of conventional columns include their big size, high consumption of solvent, high energy requirement for solvent regeneration in the stripper, and high solvent degradation and lost.

Following valuable attempts, a new approach known as high gravity technology (or Higee) was proposed by Ramshaw and Mallinson [6] to enhance the mass transfer flux between gas and liquid in the special device called rotating packed bed (RPB). There are a wide range of studies on the removal of CO_2 from

flue gases by various aqueous amine solutions in RPB. Lin et al. [7-9] have studied CO_2 removal by a cross-flow RPB using alkanolamine and sodium hydroxide (NaOH) solutions. Yu et al. [10] have investigated CO_2 capture by piperazine (PZ) and diethylene glycol (DEG) in RPB and reported overall mass transfer coefficients. Guo et al. [11] and Neumann et al. [12] have conducted experiments for CO_2 absorption by NaOH solutions to estimate the mass transfer area. The number of the modellings to evaluate the behavior and pattern of CO_2 removal by amine solutions in RPB is limited and only few studies have simulated the absorption of CO_2 in an RPB using single amine solutions. Qian et al. [13] have modelled CO_2 capture by methyldiethanolamine (MDEA) in RPB using Fortran. Kang et al. [14] and Borhani et al. [15] have developed the first principle models for CO_2 removal by monoethanolamine (MEA) using gPROMS. Joel et al. [16] have assessed such simulation for CO_2 absorption by MEA using the combination of Aspen Plus and Fortran and reported that the equipment size can be reduced by approximately 10 times when RPB is used instead of conventional columns.

The aim of this study is to model the CO_2 absorption in RPB using the blended solution of PZ and MDEA. In order to validate the proposed model, the experimental CO_2 absorption data presented by Zhan et al. [17] using the blended amine solutions of PZ + MDEA in an RPB at Beijing University of Chemical Technology (BUCT) was utilized. The model was developed by integrating MATLAB and Aspen Plus softwares. All the required correlations for the RPB, main governing equations (mass and energy balances) and some other important formulas were written in MATLAB as one of the most flexible, available and practical code-writing platforms, while the required physical and transport properties were extracted from Aspen Plus with an extreme databank in such a way that the models of PC-SAFT and E-NRTL were applied under different operating conditions for the estimation of CO_2 removal efficiency.

2. Importance of CO_2 Absorption by PZ + MDEA Solution

The application of blended amine solutions has recently attracted much attention owing to the complementary advantages of each of the amines in solution; in such a way that the primary or secondary amines have fast reactivity and absorption while the tertiary or sterically hindered alkanolamines (SHA)

have shown high absorption equilibrium capacity and low solvent stripping cost. In fact, all the equilibrium solubility, mass transfer and chemical kinetics features influence capability of a solvent to remove CO_2 [18]. The removal of CO_2 from the process gases such as natural gas, coke-oven gas and various synthesis gases by PZ + MDEA solution, which was patented by BASF, is currently adopted in some industrial operations. PZ is a cyclic symmetric diamine and contains two amino groups, so each mole of PZ is theoretically able to remove two moles of CO_2 and PZ may intensify rapid formation of carbamates. CO_2 first reacts with PZ to form zwitterions, which will be deprotonated to produce PZ-carbamate that is transferred into MDEA rapidly. PZ can be considered as a catalyst that accelerates the CO_2 absorption by MDEA [17]. The other benefits of using PZ include higher resistance to oxidative and thermal degradation compared to the primary and secondary amines. MDEA also exhibits the advantages such as resistance to degradation, suitable for the application in concentrations up to 60wt%, less corrosive and thus provides less solvent loss [19]. In the reaction mechanism of CO_2 with aqueous solutions of PZ + MDEA, the reaction of CO_2 with PZ is retreated as the rapid pseudo-first-order reaction in parallel with that of CO_2 with MDEA [20]. The primary amines are more corrosive than the secondary amines, which are more corrosive than tertiary amines according to the experimental researches. To some extent, MDEA is different from the other conventional amines because it does not create degradation products [21].

Both mass transfer and chemical reaction have a remarkable impact on the reactive absorption process and must be taken into account in the absorption model. It should be noted that one of the main methods to account for the overall reaction kinetics in the liquid phase layer is the application of enhancement factor. Because the liquid phase mass transfer resistance is crucial to CO_2 removal process [15]. Generally, enhancement factor depends on several factors such as the type of reaction, order of chemical reaction, chemical kinetics, liquid composition, physical and transport properties of the components in the liquid, stoichiometry and mass transfer model. The slowest or kinetically controlled reaction is usually considered for the enhancement factor estimation. The equilibrium and kinetic reactions of PZ and MDEA with CO_2 in addition to all the parameters and coefficients necessary to simulate CO_2 absorption by this blended amine solution in Aspen Plus have been extensively discussed by Esmaeili et al. [21, 22].

3. Model Development of RPB

In a conventional column, liquid flows under the influence of gravitational acceleration which dictates liquid and gas throughput and mass transfer rates. RPBs work with a much higher acceleration (100-1000 times of gravity) in exchange for the gravitational acceleration to increase mass transfer rate. Actually, downward liquid flow and upward gas flow due to gravity and density difference in conventional packed beds are replaced with liquid outward flow and gas inward flow in RPB. This feature allows the apparatus size significantly reduces compared to a conventional packed column for a certain type of separation. This size reduction which is cost-saving, space-saving and easy installation, results from higher volumetric mass transfer coefficients as well as intensified momentum and heat transfer rates because the formation of smaller droplets and thinner liquid films in RPB leads to higher specific surface area and enhanced mass transfer and micro-mixing efficiency compared to the conventional packed columns. In addition, the flooding limit in RPB increases, allowing operation in higher gas flow rate, more liquid hold-up and shorter residence time [23]. Due to the short residence time in RPB, this technique is suitable for the cases that require short contact time such as CO_2 absorption by PZ on account of fast reactivity. A schematic of RPB is depicted in Figure 1.

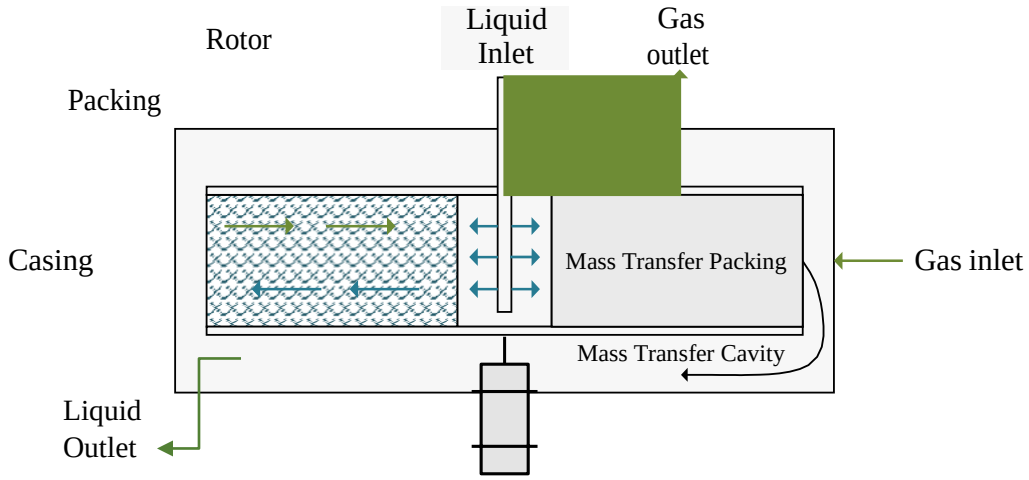

Figure 1. Schematic of a rotating packed bed

The high speed of rotation in RPB brings about small liquid droplets and finally rise in gas-liquid interfacial area and mass transfer rate. Separation in an RPB is carried out as radial counter-current flow, not vertical flow as what occurs in the conventional column operations. This feature means the separation extent is estimated by rotor radial width ($r_o - r_i$) while its capacity is constrained by axial height (h), in contrast to the conventional columns where diameter determines capacity and column height estimates separation extent.

The process intensification (PI) is a concept that aims to increase heat and mass transfer characteristics, resulting in better interaction between two fluids. The advantage of rapid mixing properties can increase the heat and mass transfer rates. Thus, systems with limitations in mixing, reaction times, and heat and mass transfer can significantly benefit from PI [24]. In CO_2 absorption process, the choice of kinetic model has a notable impact on the absorption efficiency; moreover, liquid phase mass transfer resistance is crucial and thus enhancement factor should be applied. There are different mass transfer theories to model RPB with their own model equations and approach, such as Higbie's penetration theory and the two-film theory [15]. The two-film theory, which has been widely used in the modeling of CO_2 absorption by amine solutions in RPB [14, 15, 16], has been employed in this study.

3.1. Model Assumptions, Mass and Energy Balances

The following assumptions have been considered to model CO_2 absorption by the blended amine solution of PZ + MDEA in the RPB using the mass and energy balances encrypted in MATLAB. In this study, the rotor of the RPB has been divided in to ten identical elements since the radial width of the RPB is very short and a greater number of discretization does not make notable effect on solving the gradients; furthermore, the mass and energy balances were solved for each element simultaneously. In this method of modeling, one initial guess for the outlet CO_2 concentration from the inner radius was considered as a preliminary value of CO_2 in contact with the fresh amine solution in the first element because the outlet CO_2 content is not known and should be determined by the solver using the required increments. Then, the

model estimated the CO_2 concentration in the outer radius and compared the achieved value with the inlet concentration of CO_2 into the RPB from the outer radius. If there was a high deviation, the initial guess was varied and the calculation began once more in such a way that the number of increments was controlled by the solver to obtain the specific deviation and convergence. Therefore, the results are independent of the number of discretized elements. Figure 2 indicates the schematic of rotor at RPB in radial distance with the discretized elements.

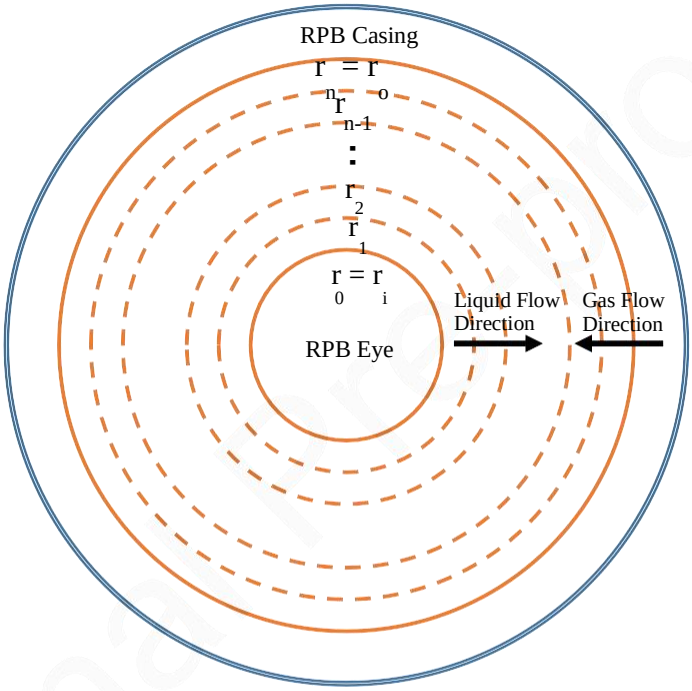

Figure 2. Schematic of rated-based modeling of the RPB in radial direction

The overall mass transfer coefficient and the difference between the partial pressures are used to calculate the mass transfer flux based on the two-film theory which is applied to the mass balances to calculate CO_2 concentration in the gas and liquid phases along radial direction.

$$N_A = K_G.P(y_{CO2} - y^*_{CO2}) \quad (1)$$

The assumptions are as follows:

1. An ideal gas phase.
2. No accumulation in gas and liquid films (steady state model).

3. Mass transfer fluxes of components between gas and liquid phases are allowed in both directions.
4. Because liquid and gas have little circumferential motion, both streams flow only in the radial direction.
5. All the reactions take place in the liquid phase.
6. Gas–liquid contact mostly occurs between r_i (inner radius of RPB) and r_o (outer radius of RPB) and the end effect has been considered.
7. The components in the gas phase are CO_2, water and amine (PZ, MDEA) and an inert gas (assumed to be N_2) and the components in liquid phase are CO_2, water and amine as well as the ionic species (hydroxyl, hydroxide, carbonate, bicarbonate, amine carbamate and protonated amine).
8. For simplicity, it is supposed that the flux of ionic species is zero and only mass transfer flux of CO_2 and amine is considered and can be estimated using the mass transfer correlations. The resistance to mass transfer for water and the amine solution of PZ + MDEA in the liquid phase is also assumed to be negligible.

In order to model the RPB in this study, all the required mass and energy balances in addition to the specific correlations of an intensified absorber were written in MATLAB and the physical and transport properties involved in each equation such as density, viscosity, surface tension, etc. were extracted from Aspen Plus which was linked to MATLAB to reduce the probable discrepancies compared with using a RadFrac extension in Aspen Plus and replacing the correlations of conventional columns with that of RPB. This method makes more flexibility to use various correlations recommended in the literature for the estimation of local-phase mass transfer coefficients in RPB while only physical and transport properties were summoned from Aspen Plus where does not exist any model for RPB simulation. The mass and energy balances for both liquid and gas phases with the relevant boundary conditions based on molar flows in RPB are as follows. The equations of 3, 5, 7 and 10 are the solution of each of mass and energy balances in the gas and liquid phases.

A. Mass Balance for Gas Phase

$$\frac{\partial(y_i.F_G)}{\partial r}\frac{1}{2\pi rh} = \varepsilon.a.N_i \qquad (2)$$

B.C.: $y_i = y_o \quad at \quad r = r_o$; $\quad \frac{\partial(y_i.F_G)}{\partial r} = 0 \quad at \quad r = r_i$

$$y_{ro} = y_{ri} - \frac{\varepsilon.a.N_i.\pi.h.(r_i^2 - r_o^2)}{F_G} \qquad (3)$$

B. Mass Balance for Liquid Phase

$$\frac{\partial(x_i.F_L)}{\partial r}\frac{1}{2\pi rh} = \varepsilon.a.N_i \quad (4)$$

B.C.: $x_i = x_o$ at $r = r_i$; $\frac{\partial(x_i.F_L)}{\partial r} = 0$ at $r = r_o$

$$x_{io} = x_{ii} + \frac{\varepsilon.a.N_i.\pi.h.(r_o^2 - r_i^2)}{F_L} \quad (5)$$

C. Energy Balance for Gas Phase

$$\frac{\partial(F_G.c_{pG}.T_G)}{\partial r}\frac{1}{2\pi rh} = \varepsilon.a.q_G \quad (6)$$

B.C.: $T_G = T_{G,0}$ at $r = r_o$; $\frac{\partial(F_G C_{pG} T_G)}{\partial r} = 0$ at $r = r_i$

$$T_{Go} = T_{Gi} - \frac{\varepsilon.a.q_G.\pi.h.(r_i^2 - r_o^2)}{F_G.c_{pG}} \quad (7)$$

$$q_G = h_{GL}(T_L - T_G) \quad (8)$$

D. Energy Balance for Liquid Phase:

$$\frac{\partial(F_L.c_{pL}.T_L)}{\partial r}\frac{1}{2\pi rh} = \varepsilon.a.q_L \quad (9)$$

B.C.: $T_L = T_{L,0}$ at $r = r_i$; $\frac{\partial(F_L C_{pL} T_L)}{\partial r} = 0$ at $r = r_o$

$$T_{Lo} = T_{Li} + \frac{\varepsilon.a.q_L.\pi.h.(r_o^2 - r_i^2)}{F_L.c_{pL}} \quad (10)$$

$$q_L = h_{GL}(T_L - T_G) - \Delta H_{abs} N_{CO_2} - \Delta H_{vap} N_{H_2O} \quad (11)$$

$$h_{GL} = k_G.RT_G\left(\frac{c_{PG}.\rho_G}{MW_{avg}}\right)^{1/3}\left(\frac{\lambda_G}{D_{G,avg}}\right)^{2/3} \quad (12)$$

3.2. The Required Correlations for the Modeling of RPB

The required correlations used to model the RPB were prepared in one organized order to explain the modeling step by step. The relationship between the overall mass transfer coefficient and the individual-phase (liquid and gas) mass transfer coefficients for each element can be given as follows [1].

$$\frac{1}{K_G.a} = \frac{R.T_G}{k_G.a} + \frac{H}{\Gamma . k_L.a} \quad (13)$$

It must be mentioned that the mass transfer at the interface of a two-phase system can be described by the two-film theory. The term of overall volumetric mass transfer coefficient ($K_G.a$) as a function of the absorbent concentration, CO_2 concentration, rotational speed, gas flow rate and liquid flow rate, is normally used to express experimental mass transfer coefficients of packing, whereas the effective interfacial area for mass transfer is less than the actual surface area of the packing [1]. Because the effective interfacial surface area (a) between the liquid and vapor phases is usually unknown, it is difficult to distinguish mass transfer coefficients from volumetric mass transfer coefficients ($k_G.a$ and $k_L.a$) [25].

In addition to mass transfer coefficients of gas and liquid sides, the factor of I which is called enhancement factor is defined as liquid mass transfer coefficient ratio with and without chemical reaction for CO_2 chemical absorption using sodium hydroxide and amine solutions [1]. In general, I is a strong function of amine concentration and effective interfacial area of packing as well as of the reaction mechanism in the liquid film and is used in the equation of overall volumetric mass transfer coefficient to represent the contribution of the chemical reactions of CO_2 with the solution of PZ + MDEA in mass transfer flux [26].

The above-mentioned correlation is used as a key correlation for the modeling of RPB to estimate the mass transfer of gas and liquid phases along radial direction in each discretized element. The differential mass balance for the liquid phase is integrated outward from the inner radius to the outer radius until the desired level of separation is obtained [27]. Two essential factors that characterize the mass transfer behavior and are used in the design of Higee units include effective interfacial area for mass transfer and the local-phase

volumetric mass transfer coefficients. In the following, the most important correlations to calculate the parameters contributed to overall volumetric mass transfer coefficient in RPB are discussed.

A. Gas-Phase Mass Transfer Coefficient

There are two applicable correlations which are commonly used to estimate the gas-phase mass transfer coefficient (k_G) in RPB. The first one was developed by Onda et al. [28] for gas absorption, desorption and vaporization in packed columns assuming that the wetted surface on random packing pieces such as Raschig and Berl saddles is identical with the gas-liquid interface.

Chen et al. [29] also presented an empirical equation for the calculation of gas-phase volumetric mass transfer coefficient ($k_G\, a$) in an RPB using the two-film theory with considering the end effect. It has been shown that the local gas-side mass transfer coefficient is related to the flow rates of gas and liquid phases, the centrifugal acceleration and the liquid viscosity [29]. The CO_2 diffusivity in gas phase is estimated by the proposed correlation of Fuller et al. [30]:

$$\frac{k_G.\,a}{D_G.\,a_t^2}\left(1-0.9\frac{V_o}{V_t}\right)=0.023\,Re_G^{1.13}.\,Re_L^{0.14}.\,Gr_G^{0.31}.\,We_L^{0.07}.\left(\frac{a_t}{a'_p}\right)^{1.4} \tag{14}$$

$$D_{G,A}=\frac{1-y_A}{\sum_{B=1}^{n}\left(\frac{y_B}{D_{G,AB}}\right)} \tag{15}$$

$$D_{G,AB}(m^2/s)=\frac{1.43\times10^{-5}T^{1.75}\left(\frac{1}{MW_G}+\frac{1}{MW_i}\right)^{0.5}}{P\times\left[\left(\sum_A v_i\right)^{1/3}+\left(\sum_B v_i\right)^{1/3}\right]^2} \tag{16}$$

In this equation, a'_p is the surface area per unit volume of 2.0-mm diameter bead (3000 m^2/m^3). It should be noted that there is a phenomenon in RPBs namely end effect. The end effect is a significant phenomenon in an RPB, resulting in the maximum mass transfer efficiency near the inner edge of the rotor. The end effect at the inner radius of RPB is caused by different factors such as the existence of the most violent collisions with the highest relative velocity between liquid jets and the packing, the strongest gas-liquid interaction with the maximum gas flux through the smallest cross-sectional area of the rotor, and fastest replenishment of fresh liquid from the liquid distributor [31].

B. Liquid-Phase Mass Transfer Coefficient

Chen et al. [32] proposed a correlation to determine the liquid-side mass transfer coefficient in rotating packed beds. Since the end effects phenomenon significantly affect $k_L a$, this factor should be considered in the correlation. Chen et al. [32] also presented that the end effects in an RPB rely on the volume inside the inner radius of the RPB (V_i), the volume between the outer radius of the RPB and the stationary housing (V_o) and the total volume of the RPB (V_t):

$$\frac{D_L}{k_L . d_p}\left(1 - 0.93\frac{V_t}{V_o} - 1.13\frac{V_t}{V_i}\right) = 0.35\, Sc_L^{0.5} . Re_L^{0.17} . Gr_L^{0.3} . We_L^{0.3} . \left(\frac{a}{a_t}\right) . \left(\frac{a'}{a_t}\right)_p^{-0.5} \left(\frac{\sigma_w}{\sigma_c}\right)^{0.14} \quad (17)$$

$$V_i = \pi . r_i^2 . h \quad (18)$$

$$V_o = \pi . \left(r_s^2 - r_o^2\right) . h \quad (19)$$

$$V_t = \pi . r_s^2 . h \quad (20)$$

D_L is CO_2 diffusivity in amine solution of PZ + MDEA, r_s and h represent radius of stationary housing and axial height of RPB respectively. This correlation covers various types of packing including ceramic beads, glass beads, acrylic beads, stainless steel beads, Raschig rings, Intalox saddles, wire meshes and hydrophobically treated beads. The above-mentioned equation is valid for various sizes of the RPBs and for viscous Newtonian and non-Newtonian liquid systems. The parameters of a'_p and σ_w are the specific surface area of the 2.0-mm bead and the surface tension of water at 25℃, whose values are 3000 m^2/m^3 and 0.072 kg/s^2 respectively.

Versteeg et al. [33] presented the following analogy to estimate CO_2 diffusivity in amine solutions where N_2O diffusivity in amine solutions is applied based on a modified Stokes-Einstein relation:

$$D_{CO_2 - H_2O}\left(\frac{m^2}{s}\right) = 2.35 \times 10^{-6} . \exp\left(-\frac{2119}{T}\right) \quad (21)$$

$$D_{CO_2 - AM} = D_{CO_2 - H_2O} \times \left[\frac{\mu_{H_2O}}{\mu_{AM}}\right]^{0.8} \quad (22)$$

C. Effective Interfacial Surface Area

The packing structure, as the core medium, is closely related to the CO_2 absorption performance of high gravity-based RPBs because it directly influences hydrodynamics and mass transfer. The packing characteristics such as material, shape, geometry, voidage, stacking arrangement and bulk density have impact on the gas-liquid flow pattern and pressure drop. Packing with a high specific surface area (a_t) and wettability assists to maintain suitable values of liquid holdup and flooding points, resulting in enhancement of gas-liquid mass transfer [5]. Wire mesh or metal foam packing is appropriate for distillation and absorption on account of high porosity (ε) and low frictional pressure drop. It is recommended that the packing provides a big surface area for mass transfer and an open structure (for low pressure drop), as well as being durable and mechanically strong enough to endure continuous rotation at high speeds with thrown-out liquid process. Metal foams appear to meet these requirements [27].

Based on the proposed correlation by Onda et al. [28], effective interfacial surface area was derived from the data of conventional packed bed in such a way that the application of this model is thus an extrapolation, the ratio a/a_t is in the range of 0.3-0.98. However, the achieved results from this correlation showed a better agreement with the real data than other equations with replacing the gravitational acceleration with the centrifugal acceleration in Froude number; furthermore, it has been used in other studies for the modeling of CO_2 absorption in RPB successfully [14,15,16]:

$$\frac{a}{a_t} = 1 - \exp\left[-1.45\left(\frac{\sigma_c}{\sigma_L}\right)^{0.75}.\mathrm{Re}_L^{0.1}.\mathrm{We}_L^{0.2}.\mathrm{Fr}_L^{-0.05}\right] \quad (23)$$

D. Enhancement Factor

Hatta number (Ha) is a key parameter to compare the rate of reaction in a liquid film to the rate of diffusion through the film. The fast reactions (Ha > 3) are taken into account to proceed predominantly near the gas-liquid interface, while the slow reactions (Ha < 3) are assumed to occur mainly in the liquid bulk [34]. For the reactions of CO_2 with PZ and MDEA, Danckwerts' correlation of enhancement factor can be used [35].

$$Ha = \frac{(D_G . k_{ov})^{1/2}}{k_L} \quad (24)$$

$$k_{ov} = k_{2,PZ}[PZ] + k_{2,MDEA}[MDEA] + k_{OH^-}[OH^-] \quad (25)$$

$$E_{CO_2} = \sqrt{1 + Ha^2} \quad (26)$$

In order to calculate the second-order reaction rate constant (k_2) of PZ and MDEA, different correlations with the various amine concentrations have been presented in the literature. The following equations are used in this study to estimate the accurate values of the first-order reaction rate for different ranges of concentration and achieve the model results compatible with the experimental data. Xu et al. [36] has proposed the second-order reaction rate constant of PZ which is valid for the concentration range of 0-0.2 kmol/m^3 and the temperature range of 303-343K.

$$k_{2,PZ}\left(\frac{m^3}{kmol.s}\right) = 2.98 \times 10^{11} . \exp\left[\frac{-6424}{T(K)}\right] \quad (27)$$

Zhang et al. [35] reported the following second-order reaction rate constant of CO_2 with PZ in the concentration and temperature limits of 0.2-0.6 mole/lit and 303-343 K respectively:

$$k_{2,PZ}\left(\frac{m^3}{kmol.s}\right) = 4.0 \times 10^{10} . \exp\left(\frac{-4059.4}{T(K)}\right) \quad (28)$$

Tertiary amines such as MDEA do not react with CO_2 directly, but act as a base that catalyzes the hydration of CO_2 (according to the base-catalyzed hydration mechanism). Haimour et al. [37] presented an equation for the second-order reaction rate constant of MDEA in the concentration domain of 0.85-1.70 kmol/m^3 and the temperature range of 288-308 K.

$$k_{2,MDEA}\left(\frac{m^3}{kmol.s}\right) = 8.741 \times 10^{12} . \exp\left(\frac{-8625}{T(K)}\right) \quad (29)$$

Sema et al. [38] exhibited the following equation for the second-order reaction rate constant of MDEA in the higher concentrations:

$$k_{2,MDEA}\left(\frac{m^3}{kmol.s}\right) = 2.661 \times 10^{11} . \exp\left(\frac{-6573}{T(K)}\right) \quad (30)$$

The second-order reaction rate constant and concentration of hydroxyl ion are calculated by the following equations [20, 39]:

$$\log_{10}(k_{OH^-}) = 13.635 - \frac{2895}{T(K)} \quad (31)$$

$$[OH^-] = \frac{K_w}{K_{p,am}}\left(\frac{1-\alpha}{a}\right), \qquad \alpha \geq 10^{-3} \quad (32)$$

$$[OH^-] = \sqrt{\frac{K_w}{K_{p,am}}[Am]}, \qquad \alpha < 10^{-3} \quad (33)$$

The required physical properties in the gas phase as well as Henry's constant and the liquid phase properties e.g. density, viscosity and heat capacity of blended amine solution of PZ + MDEA were extracted from Aspen Plus; however, the reported correlations of Paul et al. [40], Kummamuru et al. [41] and Agbonghae et al. [42] can also be used for the estimation of the above-mentioned properties in liquid phase respectively.

E. Equilibrium Partial Pressure and Heat of Absorption

For the accurate calculation of liquid-side heat transfer rate (Eq. 11), two essential parameters namely equilibrium partial pressure of CO_2 and heat of CO_2 absorption should be correlated based on the reported experimental data in the literature. To estimate the equilibrium partial pressure of CO_2 (P^*_{CO2}), the following equation which is the function of temperature and CO_2 loading is used in different concentrations of amine solution [43]:

$$P^*_{CO2} = \exp\left[A + B\alpha_{CO2} + C\ln(\alpha_{CO2}) + \frac{D}{T} + E\frac{\alpha_{CO2}^2}{T^2} + F\frac{\alpha_{CO2}}{T^2} + G\frac{\alpha_{CO2}}{T}\right] \quad (34)$$

Sakwattanapong et al. demonstrated the importance of absorption/desorption and declared that the application of constant values for heat of absorption/desorption will cause imprecise results. Therefore, the regression model for the partial pressure of CO_2 and Gibbs-Helmholtz equation can also be used to calculate the heat of absorption/desorption [43]:

$$\frac{\Delta H_{abs}}{R} = -\left[\frac{\partial \ln P^*_{CO2}}{\partial\left(\frac{1}{T}\right)}\right]_P = C\frac{\ln(\alpha_{CO2})}{T^2} - D - 2E\frac{\alpha_{CO2}^2}{T} - 2F\frac{\alpha_{CO2}}{T} + G.\alpha_{CO2} \quad (35)$$

According to the correlation (34) and the carried out regression, the following equation has been obtained to calculate the equilibrium partial pressure of CO_2 and then heat of absorption using MATLAB in a wide range of temperature (303-343 K), PZ concentration (0.041-0.21 kmol/m^3) and MDEA concentration (1.75-4.28 kmol/m^3) based on the experimental data of Xu et al. [36].

$$\mathrm{Ln}\left(P^{*}_{CO2}\right) \quad \frac{6136.711}{T} - 68591.699\frac{\alpha^2}{T^2} + 95933.471\frac{\alpha}{T^2} - 0.355C_{PZ}^{0.5} - 0.222C_{MDEA} \qquad (36)$$

F. Liquid Hold-Up

Burns et al. [44] investigated the effect of some parameters on liquid holdup in RPB. The following correlation which depends on centrifugal acceleration, liquid flow rate and liquid viscosity was presented.

$$\varepsilon_L = 0.039 \left(\frac{a_c}{g_0}\right)^{-0.5} \left(\frac{U}{U_0}\right)^{0.6} \left(\frac{\upsilon}{\upsilon_0}\right)^{0.22} \qquad (37)$$

4. Experimental Work Review

Zhan et al. [17] have conducted the experiments to study CO_2 absorption by the blended amine solutions of PZ + MDEA in an RPB with the following conditions: the solution of PZ + MDEA was introduced into the RPB by a pump through the liquid inlet and sprayed onto the inner edge of the packing and then flowed in the packing by centrifugal force. In the meantime, the gas stream containing CO_2 and H_2S flowed into the RPB through the gas inlet and passed along the packing where contacted with the amine solution countercurrently under atmospheric pressure. In this process, CO_2 and H_2S were absorbed from the gas stream into the solution through the mass transfer and certain reactions. Finally, the liquid and gas streams exited the RPB from the liquid and gas outlets respectively. All the data were collected after reaching a steady state conditions. Table 1 outlines the RPB configuration in addition to the gas and liquid operating conditions. The experimental setup of the CO_2 absorption by the blended amine solution is shown in Figure 3.

Table 1. The configuration of RPB and operating conditions of the fluids

Parameter	**Value**
Surface area per unit volume of the packing (m^2/m^3)	1533
Inner radius of the RPB, r_i (cm)	2.5
Outer radius of the RPB, r_o (cm)	7.5
Radius of the stationary housing, r_s (cm)	11.5
Axial height of the packing, h (cm)	5.3
Packing volume, V_P (cm^3)	833
Voidage of packing	0.904
Inlet CO_2 concentration, y_{in,CO_2}(%, v/v)	30
Inlet H_2S concentration, y_{in,H_2S} (%, v/v)	1
Inlet N_2 concentration, y_{in,N_2}(%, v/v)	69
Temperature, $T(K)$	302.95-318.15
High-gravity factor, β	40.0-160.0
MDEA concentration, C_{MDEA} (mole/lit)	0.84-2.94
PZ concentration, C_{PZ} (mole/lit)	0.12-0.58
Gas volumetric flow rate, Q_G (m^3/hr)	2.0
Liquid volumetric flow rate, Q_L (lit/hr)	12.6-47.6

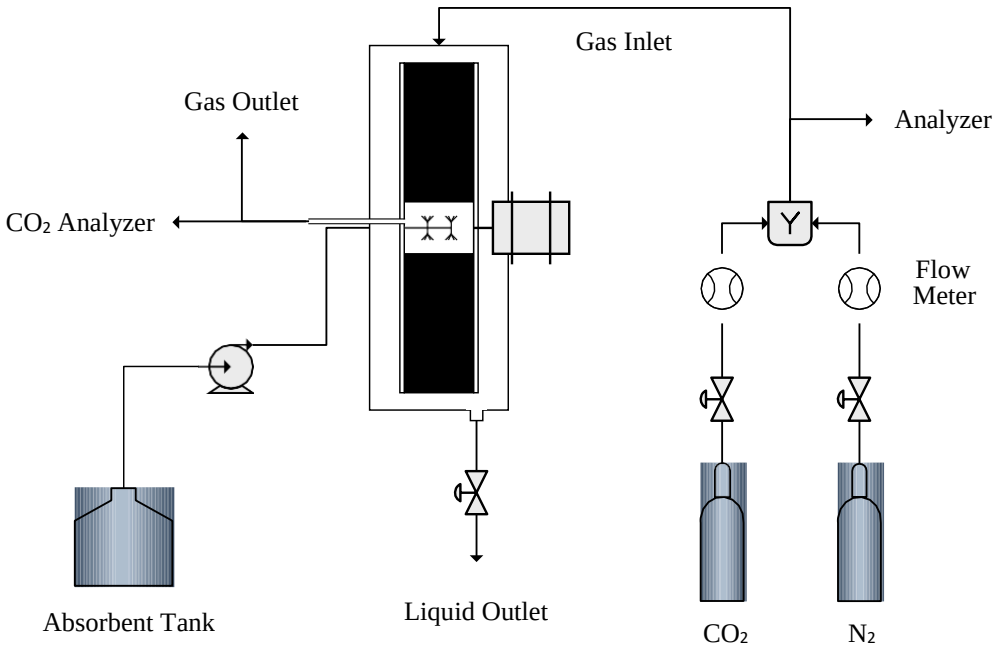

Figure 3. Schematic of experimental setup for CO_2 absorption by the blended solution of PZ + MDEA

The high-gravity factor is related to the rotational speed and is generally used to characterize the level of the high-gravity field within an RPB. It is defined as the relationship between the centrifugal acceleration ($a_c = r.\omega^2$) and the gravitational acceleration at any point in the high-gravity field. The high-gravity factor of RBP can be described using this formula [5]:

$$\beta = r.\omega^2/g = \sqrt{\frac{r_o^2 + r_i^2}{2}}.\left(\frac{2\pi N}{60}\right)^2 / 9.8 \quad (38)$$

where r (m) is the mean radius of RPB, N (r/min) is the rotational speed, and g (m/s^2) is the gravitational acceleration. Therefore, rotational speed has been considered in the range of 800-1600 rpm in the experimental works according to the data reported in Table 1.

At low high-gravity factor values, as the rotational speed increases, the CO_2 removal efficiencies enhance dramatically. However, in most cases the high-gravity factors have critical values. The factors that exceed the critical value result in stable or reduced CO_2 removal efficiencies. Before reaching the critical value, as the high-gravity factor increases, the liquid phase in RPB achieves higher speeds and leads to enhancement of the cutting and breaking effect. This effect causes thinner liquid films, finer liquid threads, and smaller liquid droplets, producing large gas-liquid contact areas and fast interface renewal. This highly brings on an increase in mass transfer and carbonation reactions between the gas and liquid phases, particularly for the fast reactions [5]. Based on the reported data of Zhan et al. [17], the most efficient high-gravity factor was $\beta = 122.5$; thus, the model was conducted by the maximum rotational speed of 1400 rpm.

The absorption efficiency ($\eta_{abs.}$) is the most important parameter for the evaluation of CO_2 removal by RPB and is defined as the percentage of carbon dioxide which is removed from inlet gas stream by the absorption process. The absorbent concentration, CO_2 concentration, rotational speed, gas-liquid flow rates, and reaction temperature are usually regarded as the key operating factors in high gravity-based absorption performance [5, 45]:

$$\eta_{abs.} = \left[1 - \left(\frac{y_{CO2,out}}{1 - y_{CO2,out}}\right)\left(\frac{1 - y_{CO2,in}}{y_{CO2,in}}\right)\right] \times 100 = 1 - \frac{Y_{CO2,out}}{Y_{CO2,in}} \quad (39)$$

Sheng et al. [4] and Liu et al. [46] exhibited the relationship between the overall volumetric mass transfer coefficient and the inlet and outlet concentrations of CO_2 in RPB, and the estimation of K_G using the measured inlet CO_2 concentration and the calculated outlet CO_2 concentration by the model in different operating conditions can be performed by the following equation.

$$G \quad m^3.Pa.s \quad \pi Ph(r_o^2 - r_i^2) \quad y_{CO2,out}(1 - y_{CO2,in}) \quad 1 - y_{CO2,in} \quad 1 - y_{CO2,out} \Big]$$

5. Model Validation and Results

As the main purpose of this study is the investigation of CO_2 removal by the blended amine solution in RPB, only modeling of CO_2 absorption into the solution of PZ + MDEA has been carried out by using MATLAB in conjunction with Aspen Plus where the relevant reactions and other required kinetics and thermodynamic parameters for CO_2 absorption were added for the estimation of desired physical and transport properties; therefore, the effect of H_2S concentration (1% v/v) was ignored and the nitrogen concentration was assumed to be 70% v/v by a reasonable approximation while the CO_2 concentration remained unchanged (30% v/v) based on the experimental conditions of Zhan et al. [17]. As earlier mentioned, the model was conducted in MATLAB by dividing the rotor of the RPB to ten differential sections with the same radial length of 0.5 cm in addition to simultaneous solving the mass and energy balances using the estimated overall volumetric mass transfer coefficient for each section (Eq. 13). In order to estimate the local-phase mass transfer coefficients and the effective interfacial surface area, the dimensionless numbers such as Reynolds, Schmidt, Weber, Grashof and Froude, which all are dependent of different physical properties should be calculated. Moreover, the temperature profile is slightly changing in the RPB due to the exothermic nature of absorption which affects the properties like density, viscosity and surface tension during the process of solving the mass and energy balances. To cope with this matter, the written code in MATLAB is connected to the model in Aspen Plus in the whole process to transport the variations into Aspen Plus and then receive new data which are used in the calculations of MATLAB. The linked model of Aspen Plus was prepared based on the reactions of PZ and MDEA with CO_2 accompanied

with the equation of states of PC-SAFT and E-NRTL to predict the physical and transport properties for the gas and liquid phases respectively (as discussed by Esmaeili et al. [22]) in the specific operating conditions. Figure 4 outlines the applied steps for the modeling and simulation of CO_2 absorption in an RPB.

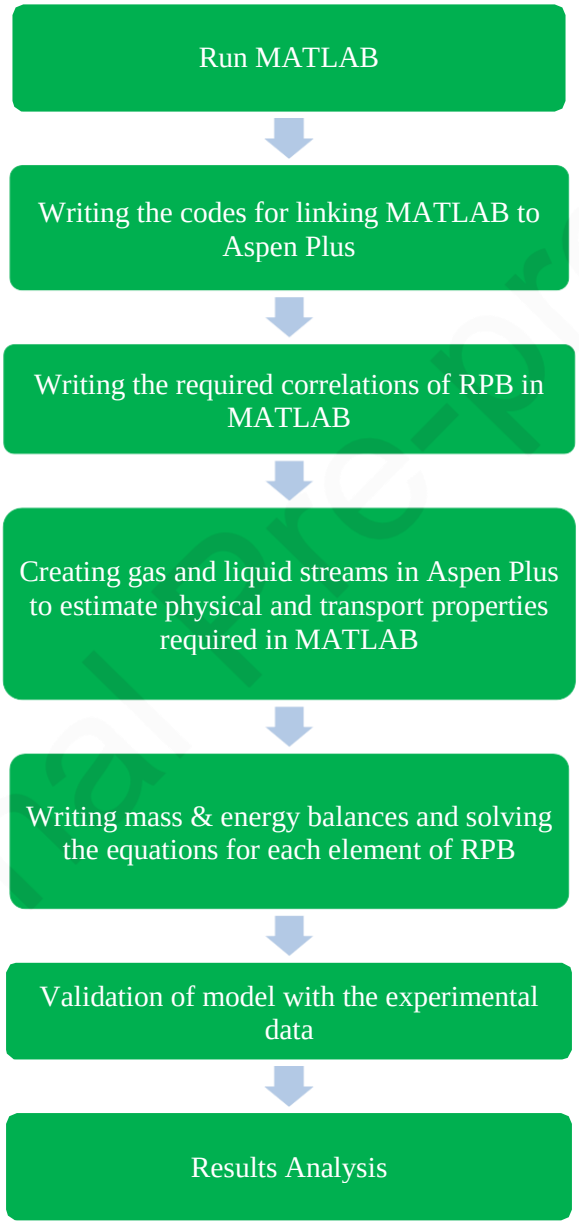

Figure 4. The applied steps of RPB modeling

The following results have been achieved by using the correlations in section 3.2 coupled with the other necessary parameters at the gas temperature of 313.15, 323.15 and 333.15 K with the gas and liquid flow

rates of 2.0 m^3/hr and 47.6 lit/hr respectively to examine the impact of various parameters on CO_2 absorption efficiency and determine the optimum operating conditions.

5.1. Effect of Rotational Speed on Absorption Efficiency

Increasing rotational speed in RPB widely causes a rise in shearing and centrifugal forces imposed on the liquid by the packing resulting in the enhancement of liquid-side mass transfer coefficient and eventually overall mass transfer coefficient (K_G) by producing smaller droplets, threads or thinner films, as illustrated in Figure 5.

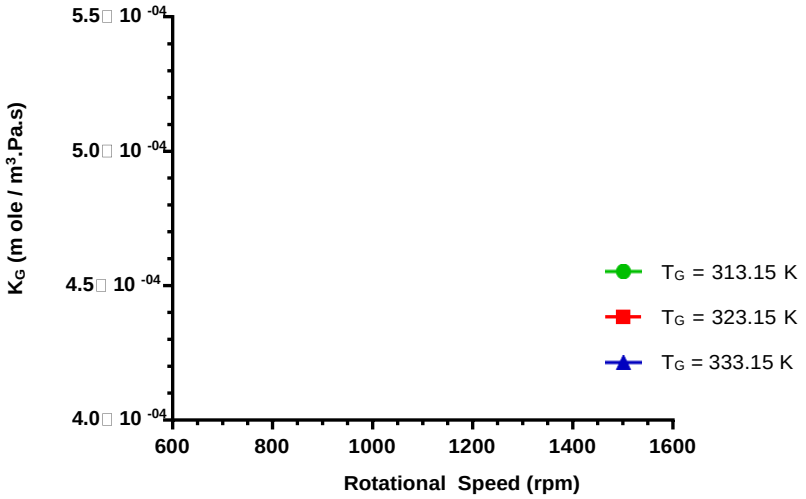

Figure 5. Variation of K_G vs. rotational speed (T_L= 313.15 K, C_{PZ}=0.35 mole/lit, C_{MDEA}=2.52 mole/lit)

The enhancement of rotational speed leads to increase in effective interfacial surface area and consequently rich-CO_2 loading, while CO_2 removal efficiency is increased and HTU (height of transfer unit) reduced. Lin et al. [47] declared that an increase in the rotational speed intensifies the mass transfer flux of CO_2 from the gas phase to the liquid phase and reduces the residence time of amine solution within RPB. When rotation is too high, CO_2 may not be entirely absorbed by the solvent in a short contact time before exiting the RPB, which weakens the CO_2 removal process further the critical speed. Therefore, amine solutions with higher reaction rates with CO_2 such as PZ or MEA are expected to be more suitable to use. Figure 6 depicts the variation of CO_2 absorption efficiency versus rotational speed in the range of 800-1400 rpm with the increments of 200 rpm, with the PZ and MDEA concentrations of 0.35 and 2.52 mole/lit

respectively, and the gas and liquid temperature of 313.15 K. An increase in the rotational speed from 800 to 1400 rpm has brought about increase in the CO_2 absorption efficiency from 79.0% to about 92.1% with the maximum AAD% (average absolute deviation) of 2.31 compared to the experimental data. As can be seen, the rise in gas phase temperature from 313.15 K to 333.15 K has not made significant effect on the amount of CO_2 removal as the main mass transfer resistance belongs to the liquid film.

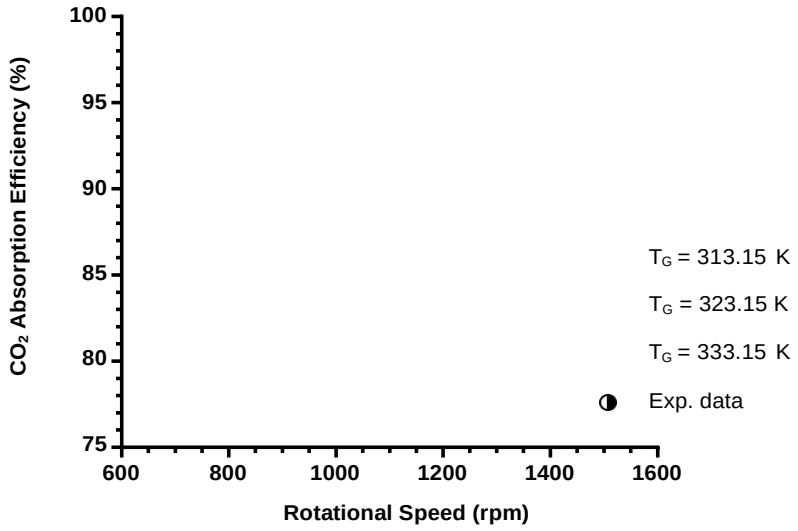

Figure 6. CO_2 absorption efficiency vs. rotational speed (T_L= 313.15 K, C_{PZ}=0.35 mole/lit, C_{MDEA}=2.52 mole/lit)

Generally, increasing lean solvent concentration brings on rise in the reaction rate between the amine solution and CO_2. On the other side, it results in an increase in the viscosity of the amine solution and Henry's constant, while CO_2 and amine molecules diffusivities in liquid phase decrease, and the overall mass transfer coefficient is thus reduced [48]. Figures 6 and 7 indicate the effect of rotational speed on CO_2 absorption efficiency at MDEA concentrations of 2.52 mole/lit and 1.68 mole/lit respectively. It can be seen from Figure 7 that the absorption efficiency has increased from 85.5 to 95.3% with enhancing rotational speed from 800 to 1400 rpm at the same temperature of 313.15 K for the gas and liquid phases with the highest AAD% of 1.19 in comparison with the experimental data. The decrease in the MDEA concentration from 2.52 mole/lit to 1.68 mole/lit has led to a slight increase in the absorption efficiency at the same rotational speed on account of the lower viscosity of the amine solution and higher ratio of PZ:MDEA (0.35:1.68). The highest absorption efficiency has occurred at the rotational speed of 1400 rpm,

which is 3.5% higher than that with the concentration ratio of 0.35:2.52 for PZ:MDEA. Therefore, increasing the total concentration of amine solution does not result in a higher absorption efficiency necessarily and the optimum concentration ratio should be found for the blended amine solutions.

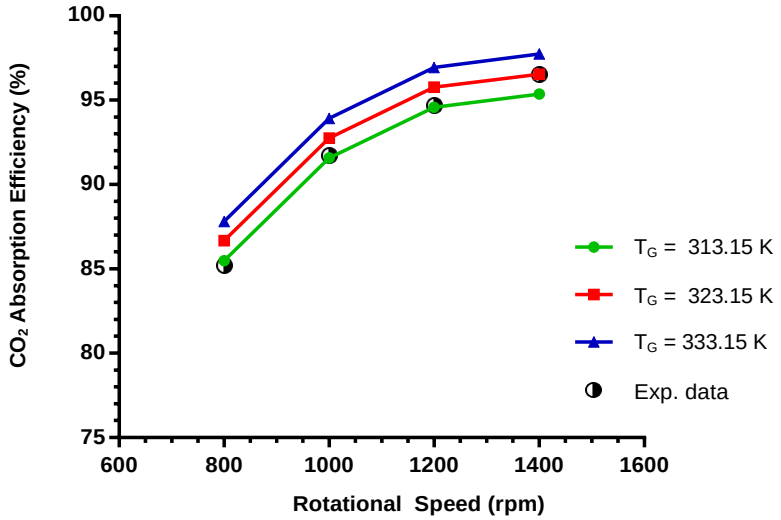

Figure 7. CO_2 absorption efficiency vs. rotational speed (T_L= 313.15 K, C_{PZ}=0.35 mole/lit, C_{MDEA}=1.68 mole/lit)

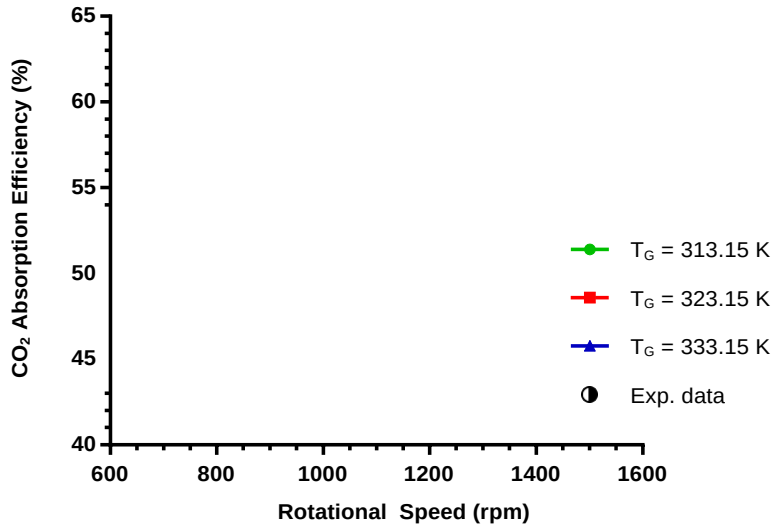

Figure 8. CO_2 absorption efficiency vs. rotational speed (T_L= 313.15 K, C_{PZ}=0.12 mole/lit, C_{MDEA}=1.68 mole/lit)

It can be seen from Figure 8 that the reduction of PZ concentration from 0.35 mole/lit to 0.12 mole/lit has caused a dramatic drop in the absorption efficiency due to the decrease of PZ (as a promoter) to MDEA ratio and the reaction rate with CO_2 compared with Figure 7. The efficiency has altered between 48.2-60.1%

with the variation of rotational speed at the same temperature of 313.15 K, and the maximum AAD% was 5.55. The modeling results clearly show that the influence of PZ on CO_2 absorption is much greater than MDEA because $k_{2,PZ}$ is at least two orders of magnitude higher than $k_{2,MDEA}$. Figures 9 and 10 demonstrate the profile of CO_2 concentration in the gas phase from the outer radius to the inner radius of the RPB at various rotational speeds in contact with the amine solutions of 0.35 mole/lit PZ and 2.52 mole/lit MDEA as well as 0.12 mole/lit PZ and 1.68 mole/lit MDEA in such a way that the highest absorption efficiency of 92.1 and 60.1% and the lowest outlet CO_2 mole concentration of 3.2 and 14.0% respectively were achieved at 1400 rpm and the same temperature of 313.15 K for both gas and liquid phases.

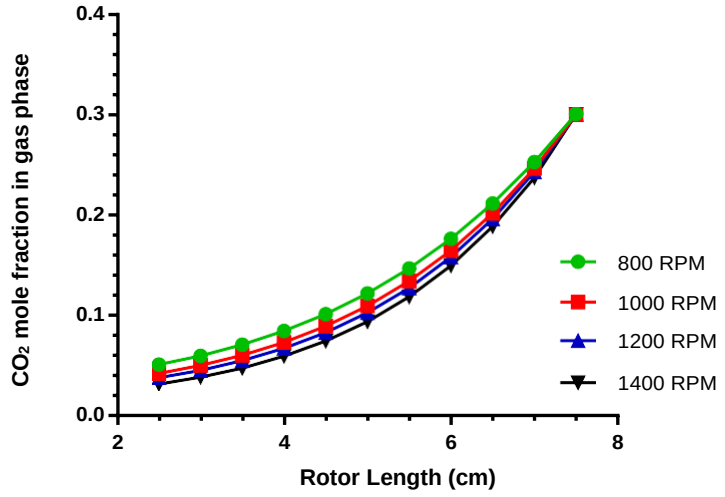

Figure 9. CO_2 concentration vs. rotor length in various rotational speeds (C_{PZ}=0.35 mole/lit, C_{MDEA}=2.52 mole/lit)

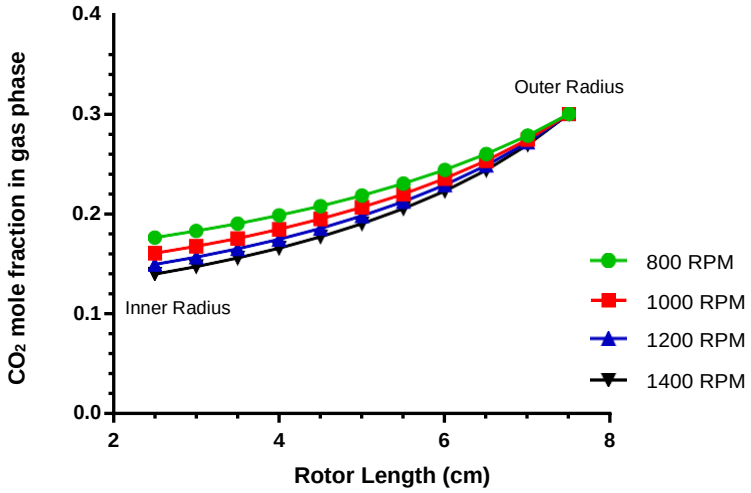

Figure 10. CO_2 concentration vs. rotor length in various rotational speeds (C_{PZ}=0.12 mole/lit, C_{MDEA}=1.68 mole/lit)

5.2. Effect of PZ and MDEA concentrations on Absorption Efficiency

According to the carbonation reaction kinetics and the classic two-film theory, the presence of CO_2 absorbents (regardless of their strong alkaline or alcoholamine characteristics) in high concentration can improve mass transfer and forward reaction kinetics in the liquid side, thus leading to an increase in CO_2 removal efficiencies. Generally, rise in the promoter (PZ) concentration brings on increase in the reaction rate between the amine solution and CO_2, the overall mass transfer coefficient (K_G) and CO_2 absorption efficiency ($\eta_{abs.}$) as shown in Figures 11 and 12. Therefore, K_G has increased as much as 2.84 times and $\eta_{abs.}$ has enhanced from 58.1% to 93.0% from the PZ concentration of 0.12 mole/lit to 0.58 mole/lit. The modeling results revealed a good agreement with the experimental data in a way that CO_2 absorption efficiency significantly increased with the variation of PZ concentration from 0.12 to 0.35 mole/lit while a further increase in PZ concentration changed the main control step to mass transfer of CO_2 instead of the reaction between CO_2 and the solution [16] which has led to a slight variation in $\eta_{abs.}$ with the highest of value of 93.0% at the similar temperature of 313.15 K for both streams and the maximum AAD% of 6.64 compared with the experimental data. The MDEA concentration is usually kept about 3-4 mole/dm^3 and a maximum PZ concentration of about 1.0 mole/dm^3 is normally applied [22].

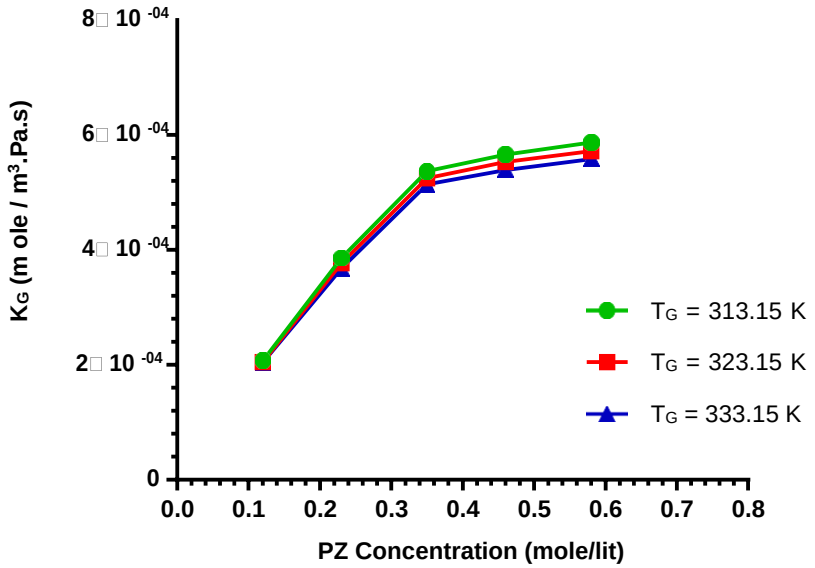

Figure 11. Variation of K_G vs. PZ concentration (T_L= 313.15 K, N=1400 rpm, C_{MDEA}=2.52 mole/lit)

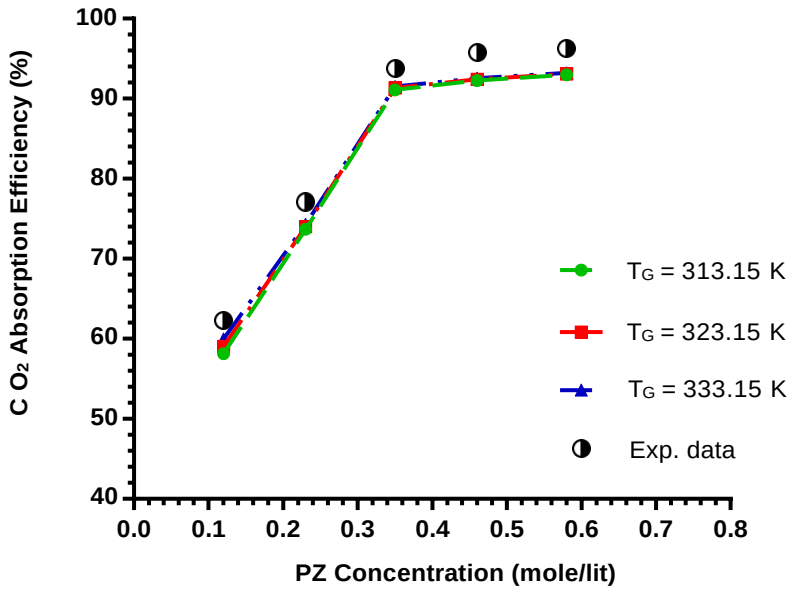

Figure 12. CO_2 absorption efficiency vs. PZ concentration (T_L= 313.15 K, N=1400 rpm, C_{MDEA}=2.52 mole/lit)

Figure 13 shows that increase in MDEA concentration has caused the initial enhancement in mass transfer, K_G and consequently $\eta_{abs.}$ up to a specific concentration because higher ratio of amine solvent per unit mass of gas and equilibrium capacity are provided, but further rise in the MDEA concentration resulted in increase in the viscosity of the amine solution and Henry's constant, decrease in CO_2 diffusivity in liquid, and K_G was thus reduced according to the correlation [48].

Furthermore, since the reaction rate of CO_2 with MDEA is slow and retention time in RPB is very short, increase in the MDEA concentration from 0.84 to 2.94 mole/lit has brought about a drop in CO_2 loading by 66.2% and also decrease in $\eta_{abs.}$ at the optimum MDEA concentration, as exhibited in Figures 14 and 15. The modeling results show that increasing MDEA concentration has positive effect on $\eta_{abs.}$ up to 1.68 mole/lit with the highest $\eta_{abs.}$ value of 93.3% at the gas and liquid temperature of 313.15 K and the maximum AAD% of 5.08 in comparison with the experimental data where the highest $\eta_{abs.}$ of 96.5% has been obtained. It has been reported that high-viscosity solution as a result of rising MDEA:PZ ratio unavoidably decrease the diffusion of absorbent molecules in the liquid phase and has a negative impact on CO_2 absorption efficiency [17].

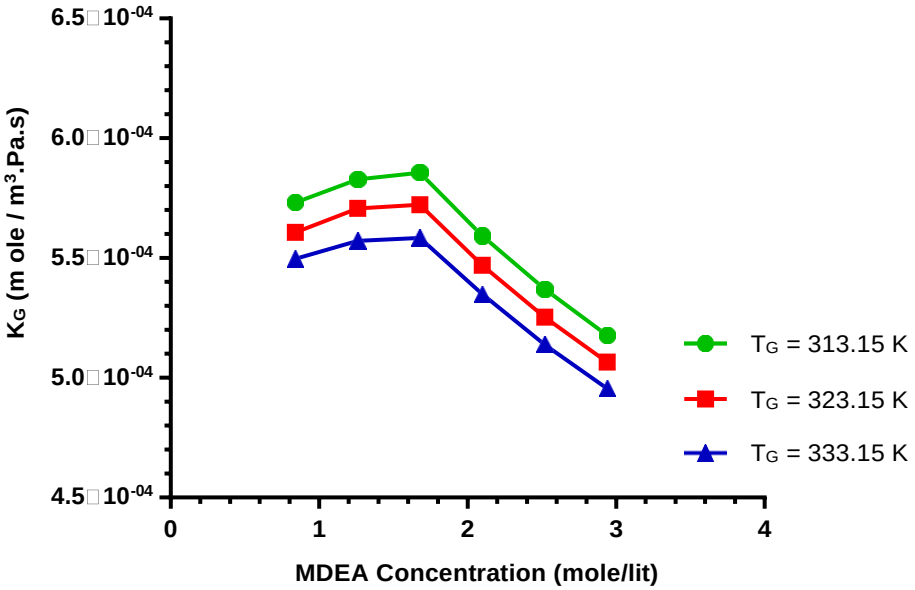

Figure 13. Variation of K_G vs. MDEA concentration (T_L= 313.15 K, N=1400 rpm, C_{PZ}=0.35 mole/lit)

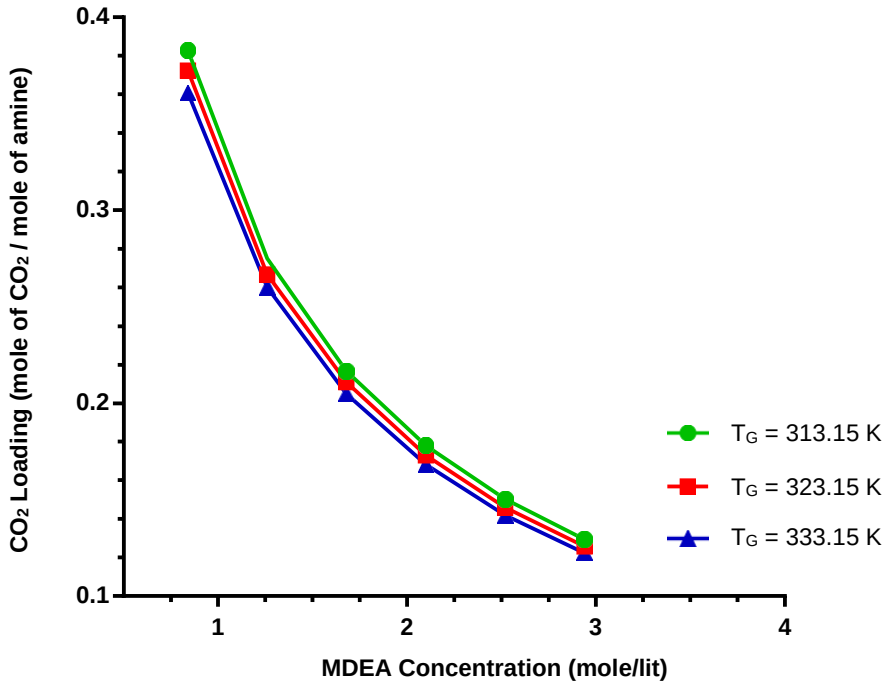

Figure 14. Variation of CO_2 loading vs. MDEA concentration (T_L= 313.15 K, N=1400 rpm, C_{PZ}=0.35 mole/lit)

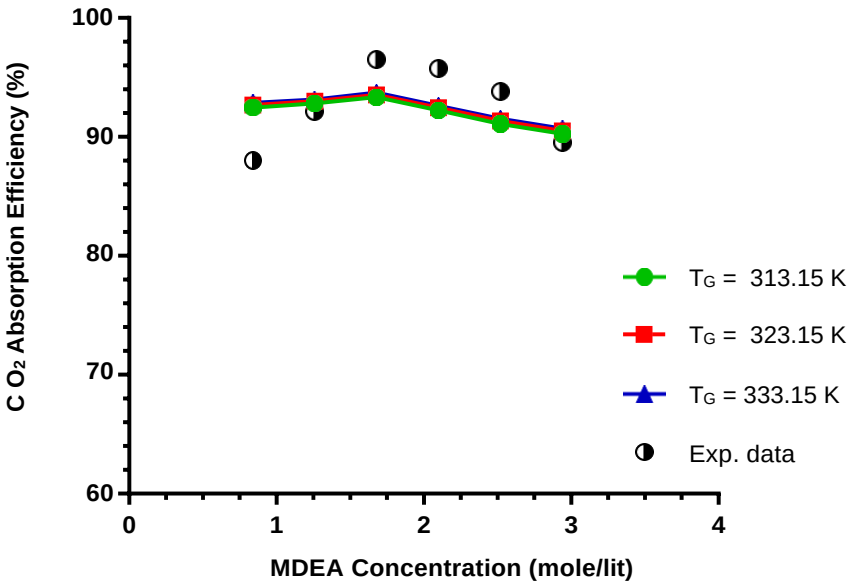

Figure 15. CO_2 absorption efficiency vs. MDEA concentration (T_L= 313.15 K, N=1400 rpm, C_{PZ}=0.35 mole/lit)

5.3. Effect of Liquid Flow Rate on Absorption Efficiency

The effect of liquid flow rate on $\eta_{abs.}$ was investigated at the limit of 30-47.6 lit/hr, with the rotational speed of 1400 rpm, MDEA concentration of 2.52 mole/lit, and temperature of 313.15 K while the PZ concentration was varied in the range of 0.12-0.58 mole/lit. As one of the most critical parameters for calculating absorption rate in a packed column, liquid flow rate plays an important role in CO_2 absorption [22]. Increasing liquid velocity (flow rate) has affected the values of Weber and Reynolds numbers significantly and led to an increase in gas-liquid contact area as the effective interfacial surface area in RPB and consequently a rise in liquid-side and overall mass transfer coefficients in such a way that the flow rates of 39 and 47.6 lit/hr have caused the higher effect on K_G than the flow rate of 30 lit/hr as shown in Figure 16. Moreover, a higher liquid flow rate provided more absorption solution per unit mass of gas to absorb higher amount of CO_2, and resulted in higher mass transfer and reaction rate between CO_2 and the amine solution and the enhancement of $\eta_{abs.}$ at the same temperature of 313.15 K for both gas and liquid phases as illustrated in Figure 17. With the increase in the liquid flow rate at a constant gas flow rate, the irrigation

rate of packing surface is increased, and the equilibrium partial pressure of CO_2 in the liquid phase is reduced. In other words, the driving force for CO_2 absorption was strongly intensified [49].

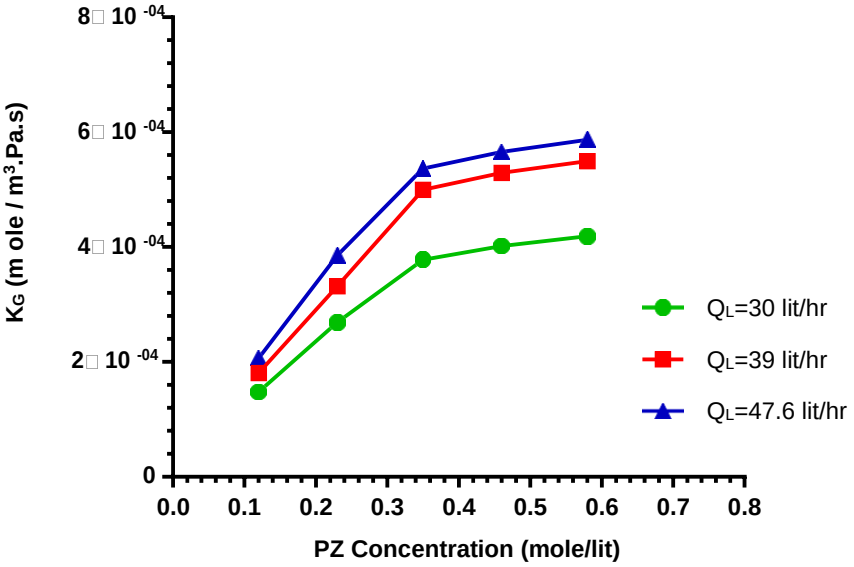

Figure 16. Variation of K_G vs. PZ concentration and liquid flow rate (T_L= 313.15 K, N=1400 rpm, C_{MDEA}=2.52 mole/lit)

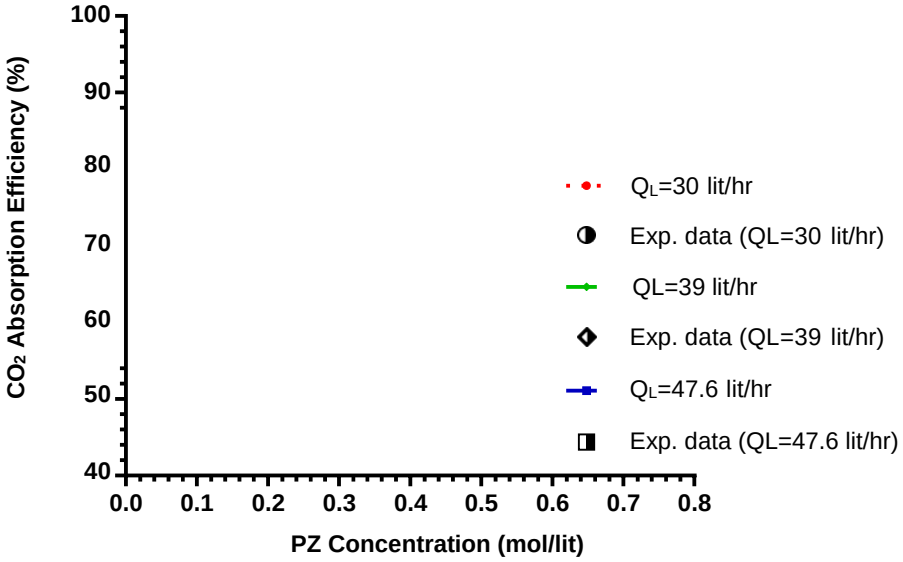

Figure 17. Variation of $\eta_{abs.}$ vs. PZ concentration and liquid flow rate (T_L= 313.15 K, N=1400 rpm, C_{MDEA}=2.52 mole/lit)

However, high liquid flow rate may cause a decrease in liquid residence time and even flooding may happen in RPB. The simulation results revealed that the rise in liquid flow rate has greater impact on $\eta_{abs.}$ in the lowest PZ concentration (0.12 mole/lit) alongside the increase from the liquid flow rate of 30 lit/hr to 39 lit/hr for all the studied PZ concentrations while there is no much difference in the amount of $\eta_{abs.}$ where the concentrations of 0.46 and 0.58 mole/lit with the flow rates of 39 and 47.6 lit/hr were used. The maximum AAD% of 6.64 has been achieved at the PZ concentration of 0.12 mole/lit and liquid flow rate of 47.6 lit/hr. For the optimum PZ concentration of 0.35 mole/lit, $\eta_{abs.}$ has increased by 10.2 and 1.84% with the increment of 9 lit/hr in the liquid flow rate.

5.4. Effect of Liquid Temperature on Absorption Efficiency

It is known that equilibrium absorption capacity is decreased with increasing liquid temperature according to the exothermic nature of absorption and also leads to an increase in reaction rate according to the Arrhenius equation of the second-order reaction rate constant [2]. Generally, rising liquid temperature promotes the second-order reaction rate constant and Hatta number while reduces the viscosity of amine solution and thus the liquid film thickness because the ratio of viscosity to density (kinematic viscosity) can be the controlling factor which determines the film thickness [16]. All the mentioned factors favor the mass transfer process and eventually lead to an increase in K_G, as depicted in Figure 18. The results exhibit that CO_2 absorption efficiency increased with rise in amine solution temperature, suggesting that an enhancement in reaction rate played a more significant role in CO_2 removal than a decrease in equilibrium capacity at higher temperatures for the solution of PZ + MDEA. A rise in temperature brings about an increased number of activated molecules and effective collision frequency which intensifies the reaction rate according to the reaction dynamics. However, the enhancement in temperature leads to increase in CO_2 partial pressure and lowers the gas solubility, causing a reduction in the mass transfer driving force. Furthermore, the reaction between PZ with CO_2 is exothermic and thus much higher temperatures accelerates the reverse reaction.

As a result, the effect of temperature has a combined outcome, resulting in optimal temperature values in the range of 313-318 K. It has been reported that CO_2 removal level enhances remarkably in the temperature domain of 25 ℃ to 50 ℃ of lean amine solution but further increase above 50 ℃ has no significant effect on the CO_2 removal level [50]. Figure 19 demonstrates the variation of $\eta_{abs.}$ with the rise in the liquid temperature from 303 K to 318 K coupled with the rotational speed of 1400 rpm and the PZ and MDEA concentrations of 0.35 and 2.52 mole/lit respectively. The simulation results have shown a good agreement compared to the experimental data in a way that $\eta_{abs.}$ has increased from 86.1 to 92.8% with the highest AAD% of 3.17.

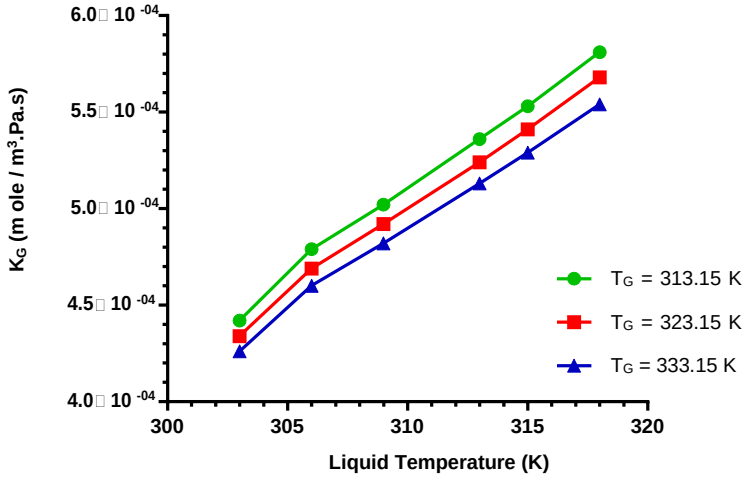

Figure 18. Variation of K_G vs. liquid temperature (N=1400 rpm, C_{PZ}=0.35 mole/lit, CMDEA=2.52 mole/lit)

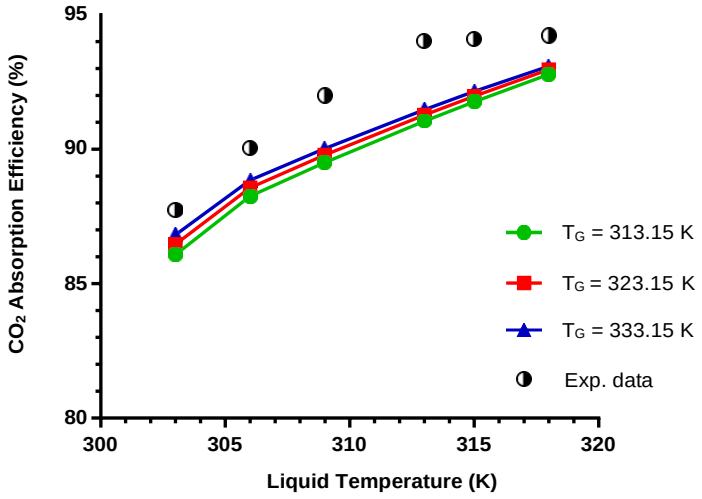

Figure 19. Variation of $\eta_{abs.}$ vs. liquid temperature (N=1400 rpm, C_{PZ}=0.35 mole/lit, C_{MDEA}=2.52 mole/lit)

5.5. Effect of Operational Parameters on Liquid Holdup

In the packed beds, the gas and liquid flow rates are limited by the tendency to flood in the column. Liquid holdup, which is the trapped liquid phase in packing and means the occupied liquid along the bed, was found to depend on liquid flow rate, rotational speed and viscosity (which is the function of temperature) in an RPB according to Eq. 37. Burns et al. [44] used an electrical resistance approach to measure the liquid holdup in an RPB and have proposed an applicable correlation which was applied to estimate the liquid holdup in the modeling of CO_2 removal using amine solutions in RPB [14,15,16]. It appeared that the liquid holdup is strongly affected by centrifugal acceleration and liquid velocity (flow rate). An increase in the liquid velocity at either constant liquid temperature or rotational speed leads to rise in liquid holdup sharply at the gas temperature of 313.15 K, as exhibited in Figures 20 and 21.

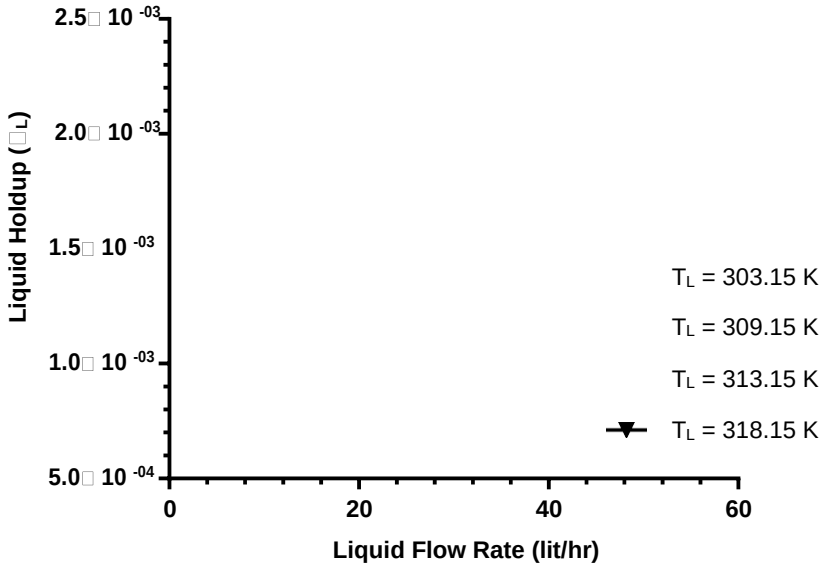

Figure 20. Liquid holdup vs. liquid flow rate (N=1400 rpm, C_{PZ}=0.35 mole/lit, C_{MDEA}=2.52 mole/lit)

On the other side, enhancing the liquid temperature results in the reduction in liquid viscosity and the slight decrease in the liquid holdup while increasing centrifugal acceleration (rotational speed) leads to the significant decrease in the liquid holdup in such a way that it decreased by 42.8% with the rotational speed

increasing from 800 rpm to 1400 rpm at the liquid flow rate of 48 lit/hr. Figure 21 demonstrates that the liquid holdup declined sharply as the rotational speed increased from 800 to 1000 rpm at the same temperature of 313.15 K for gas and liquid phases and then decreased gradually up to the rotational speed of 1400 rpm as presented by Yang et al. [51]. This could be attributed to change in the regime of the liquid flow from pore flow to film flow and then to rivulets and droplet flow, resulting in a gradual increase in tortuosity of liquid flow with rising acceleration [44]. Furthermore, reduction in liquid holdup assists gas to pass rotor easily and pressure drop decreases accordingly.

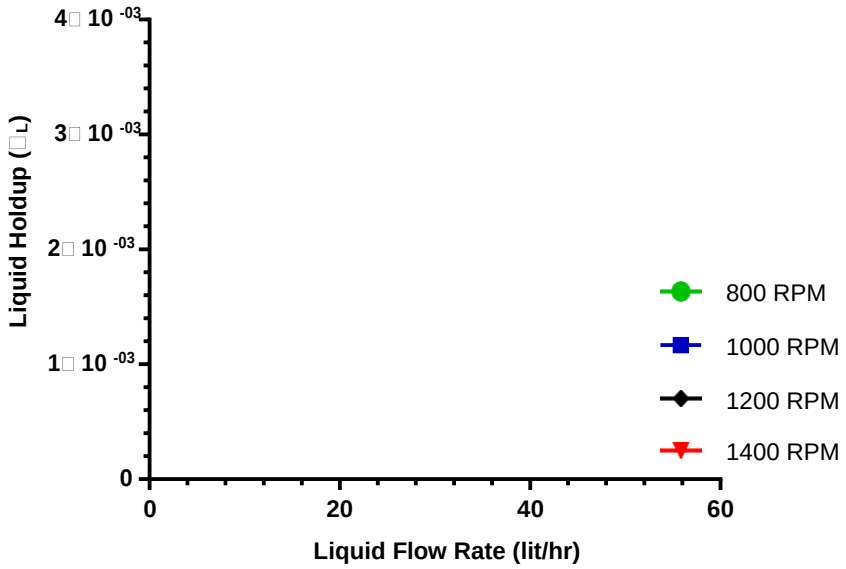

Figure 21. Liquid holdup vs. liquid flow rate (T= 313.15 K, C_{PZ}=0.35 mole/lit, C_{MDEA}=2.52 mole/lit)

6. Conclusion

In this work, the modeling of CO_2 absorption in the blended amine solution of PZ + MDEA by a rotating packed bed was conducted with the application of MATLAB linked to Aspen Plus as a rate-based steady state model and the results were validated by the experimental data in the previous study [17]. The rotor of the RPB was divided into ten differential elements with the same radial length of 0.5 cm for the determination of mass and energy balances, which were written in MATLAB and solved simultaneously to consider the impact of concentration and temperature changes on the physical and transport properties

estimated by Aspen Plus. The most applicable correlations published in the literature were used to model and calculate the required parameters; the gas-side and liquid-side mass transfer coefficients were estimated by the correlations of Chen et al. [29,32] while the proposed equation by Onda et al. [28] was employed to predict the values of effective interfacial surface area.

Different parameters such as CO_2 absorption efficiency, overall mass transfer coefficient, CO_2 loading and CO_2 concentration profile in the gas phase were obtained using the model. The simulation results indicate good agreement with the experimental data particularly with the variation of rotational speed, PZ concentration and liquid temperature among which the highest AAD% for CO_2 absorption is 6.64. Increasing rotational speed, PZ concentration, liquid temperature and flow rate has shown the continuous enhancement on CO_2 absorption efficiency while rising MDEA concentration has influenced on CO_2 removal up to an optimal concentration. Therefore, the favorite conditions have been determined as the rotational speed of 1400 rpm, PZ concentration of 0.35 mole/lit, MDEA concentration of 1.68 mole/lit, liquid flow rate of 47.6 lit/hr and liquid temperature of 313.5 K. The outcomes reveal that the kinetic model has a significant effect on the simulation data in such a way that varying the second order reaction rate constant of each amine solvent in a certain range can reduce the deviation of the model predications with the experimental data.

Acknowledgement

This work was financially supported by the National Natural Science Foundation of China (No. 22078009).

Nomenclature

Symbols Used

a	effective interfacial surface area of packing (m^2/m^3)
a_c	centrifugal acceleration (m/s^2)
a'_p	surface area of the 2-mm diameter bead per unit volume of bed (m^2/m^3)
a_t	total surface area of packing (m^2/m^3)
C_{MDEA}	methyldiethanolamine concentration (mole/lit)
c_{pG}	specific heat capacity of gas phase (J/mole.K)
c_{pL}	specific heat capacity of liquid phase (J/mole.K)
C_{PZ}	piperazine concentration (mole/lit)
D_G	diffusivity in gas phase (m^2/s)
$D_{G,avg.}$	average diffusivity in gas phase (m^2/s)
D_L (or D_{AB})	diffusivity of component i in liquid phase (m^2/s)
d_p	effective diameter of packing (m) : $6(1-\varepsilon)/a_t$
E (or I)	enhancement factor
F_G	total molar flow rate of gas phase (mole/s)
F_L	total molar flow rate of liquid phase (mole/s)
G	superficial mass velocity of gas phase ($kg/m^2.s$)
G_I	molar flow rate of inert gas (mole/s)
g	gravitational acceleration (m/s^2)
g_0	characteristic centrifugal acceleration (= 100 m/s^2)
h	axial height of packing (m)
H	Henry's constant in liquid phase ($Pa.m^3/mole$)
Ha	Hatta number
h_{GL}	gas-liquid interfacial heat transfer coefficient ($W/m^2.K$)
k_2	second-order reaction rate constant ($m^3/kmol.s$)
K_G	overall mass transfer coefficient ($mole/m^2.Pa.s$)
k_G	mass transfer coefficient in gas phase (m/s)
k_L	mass transfer coefficient in liquid phase (m/s)
k_{ov}	overall reaction rate constant (1/s)

$K_{p,am}$	protonation constant of amine solvent (kmol/m^6)
K_w	dissociation constant for water (kmol^2/m^6)
L	superficial mass velocity of liquid phase (kg/m^2.s)
$MW_{avg.}$	average molecular weight (g/mol)
N	rotational speed (rpm)
N_i	molar mass-transfer flux of component i (mole/m^2.s)
P	total pressure (Pa)
P^*	equilibrium partial pressure (Pa)
q_G	heat transfer flux in gas phase (W/m^2)
q_L	heat transfer flux in liquid phase (W/m^2)
R	universal gas constant (Pa.m^3/mole.K)
r	radius axis of RPB (m)
r_i	inner radius of RPB (m)
r_o	outer radius of RPB (m)
r_S	radius of stationary housing (m)
T	absolute temperature (K)
T_G	gas temperature (K)
T_i	temperature at inner radius of each differential element (K)
T_L	liquid temperature (K)
T_o	temperature at outer radius of each differential element (K)
U	volumetric liquid flow rate per unit area (m/s)
U_0	characteristic volumetric liquid flow rate per unit area (= 0.01 m/s)
v_i	special atomic diffusion volume
V_i	volume inside the inner radius of the RPB (m^3)
V_o	volume between the outer radius of the RPB and the stationary housing (m^3)
V_t	total volume of RPB (m^3)
x_i	mole fraction of component i in liquid phase
x_{ri}	mole fraction of component i in liquid phase at inner radius of each differential element
x_{ro}	mole fraction of component i in liquid phase at outer radius of each differential element
Y_i	molar ratio of component i in gas phase ($y_i/1-y_i$)
y_i	mole fraction of component i in gas phase

y_i^*	equilibrium mole fraction of component i at gas-liquid interface
y_{ri}	mole fraction of component i in gas phase at inner radius of each differential element
y_{ro}	mole fraction of component i in gas phase at outer radius of each differential element
z	stoichiometric coefficient
ΔH_{abs}	heat of absorption (J/mol)
ΔH_{vap}	heat of vaporization of water (J/mol)

Greek Symbols

α	CO_2 loading
β	high-gravity factor
ε	porosity of packing (m^3/m^3)
ε_L	liquid holdup
η	efficiency
λ	thermal conductivity (W/m.K)
μ	viscosity (Pa.s)
ν	kinematic viscosity (m^2/s)
ν_0	characteristic kinematic viscosity (= 1.0×10^{-6} m^2/s)
ρ	density (kg/m^3)
σ	surface tension of liquid phase (kg/s^2)
σ_c	critical surface tension of packing material (kg/s^2)
σ_w	surface tension of water (kg/s^2)
ω	angular velocity (rad/s)

Subscripts

abs	absorption
G	gas-phase
i	inlet
L	liquid-phase
o	outlet
s	stationary housing
vap	vaporization

Dimensionless Groups

Fr_L	Froude number ($\frac{L^2.a_t}{\rho^2.q_c}$)
Gr_G	Grashof number of gas side ($\frac{d_p^3.a_c}{\nu_G^2}$)
Gr_L	Grashof number of liquid side ($\frac{d_p^3.a_c}{\nu_L^2}$)
Re_G	Reynolds number of gas side ($\frac{G}{a_t.\mu_G}$)
Re_L	Reynolds number of liquid side ($\frac{L}{a_t.\mu_L}$)
Sc_L	Schmidt number of liquid side ($\frac{\nu_L}{D_L}$)
We_L	Weber number ($\frac{L^2}{\rho_L.a_t.\sigma}$)

Abbreviations

AAD	average absolute deviation
DEG	diethyleneglycol
$E-NRTL$	electrolyte non-random two-liquid
HTU	height of transfer unit
$MDEA$	methyldiethanolamine
MEA	monoethanolamine
$NaOH$	sodium hydroxide
$PC-SAFT$	perturbed-chain statistical associating fluid theory
PI	process intensification
PZ	piperazine
RPB	rotating packed bed
SHA	sterically hindered alkanolamine

References

1. Lin, C., Liu, W., Tan. C. Removal of carbon dioxide by absorption in a rotating packed bed. *Ind. Eng. Chem. Res.* **2003**, *42*, 2381-2386.
2. Yu, C., Cheng, H., Tan, C. CO_2 capture by alkanolamine solutions containing diethylenetriamine and piperazine in a rotating packed bed. *Int. J. Greenhouse Gas Control.* **2012**, *9*, 136-147.
3. Sheng, M., Xie, C., Zeng, X., Sun, B. Intensification of CO_2 capture using aqueous diethylenetriamine (DETA) solution from simulated flue gas in a rotating packed bed. *Fuel*. **2018**, *234*, 1518-1527.
4. Sheng, M., Sun, B., Zhang, F., Chu, G. Mass-Transfer characteristics of the CO_2 absorption process in a rotating packed bed. *Energy Fuels*. **2016**, *30*, 4215-4220.
5. Zhao, B., Tao, W., Zhong, M., Su, Y., Cui, G. Process, performance and modeling of CO_2 capture by chemical absorption using high gravity: A review. *Renewable Sustainable Energy Rev.* **2016**, *65*, 44-56.
6. Ramshaw, C., Mallinson, R.H. Mass Transfer Process. U.S. Patent 4, 283,255, **1981**.
7. Lin, C., Lin, Y., Tan. C. Evaluation of alkanolamine solutions for carbon dioxide removal in cross-flow rotating packed beds. *J. Hazard. Mater.* **2010**, *175*, 344-351.
8. Lin, C., Chen, B. Carbon dioxide absorption in a cross-flow rotating packed bed. *Chem. Eng. Res. Des.* **2011**, *89*, 1722-1729.
9. Lin, C., Chen, B. Carbon dioxide absorption into NaOH solution in a cross-flow rotating packed bed. *J. Ind. Eng. Chem.* **2007**, *7*, 1083-1090.
10. Yu, C., Wu, T., Tan. C. CO_2 capture by piperazine mixed with non-aqueous solvent diethylene glycol in a rotating packed bed. *Int. J. Greenhouse Gas Control.* **2013**, *19*, 503-509.
11. Guo, K., Zhang, Z., Luo, H., Dang, J., Qian, Z. An innovative approach of the effective mass transfer area in the rotating packed bed. *Ind. Eng. Chem. Res.* **2014**, *53*, 4052-4058.
12. Neumann. K., Hunold, S., de Beer, M. Mass transfer studies in a pilot scale RPB with different packing diameters. *Ind. Eng. Chem. Res.* **2018**, *57*, 2258-2266.
13. Qian, Z., Xu, L., Cao, H., Guo, K. Modeling study on absorption of CO_2 by aqueous solutions of N-methyldiethanolamine in rotating packed bed. *Ind. Eng. Chem. Res.* **2009**, *48*, 9261-9267.
14. Kang, J., Sun, K., Wong, D., Jang, S., Tan. C. Modeling studies on absorption of CO_2 by monoethanolamine in rotating packed bed. *Int. J. Greenhouse Gas Control.* **2014**, *25*, 141-150.
15. Borhani, T.N., Oko, E., Wang, M. Process modelling and analysis of intensified CO_2 capture using monoethanolamine (MEA) in rotating packed bed absorber. *J. Cleaner Prod.* **2018**, *204*, 1124-1142.
16. Joel, A. S. Wang, M., Ramshaw, C. Modelling and simulation of intensified absorber for post-combustion CO_2 capture using different mass transfer correlations. *Appl. Therm. Eng.* **2015**, *74*, 47-53.
17. Zhan, J., Wang, B., Zhang, L., Sun, B. Simultaneous absorption of H_2S and CO_2 into the MDEA + PZ aqueous solution in a rotating packed bed. *Ind. Eng. Chem. Res.* **2020**, *17*, 8295-8303.
18. Bishnoi, S., Rochelle, G.T. Absorption of carbon dioxide into aqueous piperazine: reaction kinetics, mass transfer and solubility. *Chem. Eng. Sci.* **2000**, *55*, 5531-5543.
19. Borhani, T.N., Wang, M. Role of solvents in CO_2 capture processes: The review of selection and design methods. *Renewable Sustainable Energy Rev.* **2019**, *114*, 109299.
20. Sun, W., Yong, C., Li, M. Kinetics of the absorption of carbon dioxide into mixed aqueous solutions of 2-amino-2-methyl-1-propanol and piperazine. *Chem. Eng. Sci.* **2005**, *60*, 503-516.

21. Esmaeili, A., Liu, Zh., Xiang, Y., Yun, J., Shao, L. Simulation and validation of carbon dioxide removal from the ethane stream in the south pars phase 19 gas plant by different amine solutions using rate-based model. *J. Nat. Gas Sci. Eng.* **2021**, *93*, 104030.
22. Esmaeili, A., Liu, Zh., Xiang, Y., Yun, J., Shao, L. Modeling and validation of carbon dioxide absorption in aqueous solution of piperazine + methyldiethanolamine by PC-SAFT and E-NRTL models in a packed bed pilot plant: study of kinetics and thermodynamics. *Process Saf. Environ. Prot.* **2020**, *141*, 95-109.
23. Guo, J., Jiao, W., Qi, G., Yuan, Z., Liu, Y. Applications of high-gravity technologies in gas purifications: a review. *Chin. J. Chem. Eng.* **2019**, *27*, 1361-1373.
24. Rahimi, M., Mosleh, S. CO_2 removal from air in a countercurrent rotating packed bed, experimental determination of height of transfer unit. *Advances in Environmental Technology* **2015**, *1*, 25-30.
25. Kelleher, T., Fair, J. R. Distillation studies in a high-gravity contactor. *Ind. Eng. Chem. Res.* **1996**, *35*, 4646-4655.
26. Aroonwilas, A., Tontiwachwuthikul, P. High-efficiency structured packing for CO_2 separation using 2-amino-2-mehtyl-1-propanol (AMP). *Sep. Purif. Technol.* **1997**, *12*, 67-79
27. Agarwal, L., Pavani, V., Rao, D. P., Kaistha, N. Process intensification in higee absorption and distillation: design procedure and applications. *Ind. Eng. Chem. Res.* **2010**, *49*, 10046-10058.
28. Onda, K., Takeuchi, H., Okumoto, Y. Mass transfer coefficients between gas and liquid phases in packed columns. *J. Chem. Eng. Jpn.* **1968**, *1*, 56-62.
29. Chen, Y. Correlations of mass transfer coefficients in a rotating packed bed. *Ind. Eng. Chem. Res.* **2011**, *50*, 1778-1785.
30. Fuller, E.N., Schettler, P.D., Giddings, J.C. A new method for prediction of binary gas-phase diffusion coefficients. *Ind. Eng. Chem.* **1966**, *58(5)*, 19-27.
31. Luo, Y., Chu, G., Zou, H. Zhao, Z., Dudukovic, M. P., Chen, J. Gas-liquid effective interfacial area in a rotating packed bed. *Ind. Eng. Chem. Res.* **2012**, *51*, 16320-16325.
32. Chen, Y., Lin, F., Lin, C., Tai, C. Y., Liu, H. Packing characteristics for mass transfer in a rotating packed bed. *Ind. Eng. Chem. Res.* **2006**, *45*, 6846-6853.
33. Versteeg, G. F., van Swaaij, P. M. Solubility and diffusivity of acid gases (CO_2, N_2O) in aqueous alkanolamine solutions. *J. Chem. Eng. Data* **1988**, *33*, 29-34.
34. Derks, P.W.J., Kleingeld, T., van Aken, C., Hogendoorn, J.A., Versteeg, G.F. Kinetics of absorption of carbon dioxide in aqueous piperazine solutions. *Chem. Eng. Sci.* **2006**, *61*, 6837-6854.
35. Zhang, X., Zhang, C., Qin, S., Zheng, Z. A kinetics study on the absorption of carbon dioxide into a mixed aqueous solution of methyldiethanolamine and piperazine. *Ind. Eng. Chem. Res.* **2001**, *40*, 3785-3791.
36. Xu, G., Zhang, C., Qin, S., Wang, Y. Kinetics study on absorption of carbon dioxide into solutions of activated methyldiethanolamine. *Ind. Eng. Chem. Res.* **1992**, *31*, 921-927.
37. Haimour, N., Bidarian, A., Sandall, O. C. Kinetics of the reaction between carbon dioxide and methyldiethanolamine. *Chem. Eng. Sci.* **1987**, *42(6)*, 1393-1398.
38. Sema, T., Naami, A., Liang, Z., Shi, H. Solvent Chemistry: reaction kinetics of CO2 absorption into reactive amine solutions. *Carbon Manage.* **2012**, *3(2)*, 201-220.
39. Xiao, J., Li, C., Li, M. Kinetics of absorption of carbon dioxide into aqueous solutions of 2-amino-2-methyl-1-proponal + monoethanolamine. *Chem. Eng. Sci.* **2000**, *55*, 161-175.
40. Paul, S., Mandal B. Density and viscosity of aqueous solutions of (N-methyldiethanolamine + piperazine) and (2-amino-2-methyl-1-propanol + piperazine) from (298 to 333) K. *J. Chem. Eng. Data* **2006**, *51*, 1808-1810.

41. Kummamuru, N.B., Idris, Z., Eimer, D.A. Viscosity measurement and correlation of unloaded and CO_2-loaded aqueous solutions of N-methyldiethanolamine-piperazine. *J. Chem. Eng. Data.* **2019**, *64*, 4692-4700.
42. Agbonghae, E.O., Hughes, K.J., Ingham, D.B., Ma, L., Pourkashanian, M. A semi-empirical model for estimating the heat capacity of aqueous solutions of alkanolamines for CO_2 capture. *Ind. Eng. Chem. Res.* **2014**, *53*, 8291-8301.
43. Borhani, T.N., Oko, E., Wang, M. Process modelling, validation and analysis of rotating packed bed stripper in the context of intensified CO_2 capture with MEA. *Ind. Eng. Chem.* **2019**, *75*, 285-295.
44. Burns, J.R., Jamil, J.N., Ramshaw, C. Process intensification: operating characteristics of rotating packed beds – determination of liquid hold-up for a high-voidage structured packing. *Chem. Eng. Sci.* **2000**, *55*, 2401-2415.
45. Aroonwilas, A., Veawab, A. Characterization and comparison of the CO_2 absorption performance into single and blended alkanolamine in a packed column. *Ind. Eng. Chem.* **2004**, *43*, 2228-2237.
46. Liu, Zh., Esmaeili, A., Zhang, H., Xiao, H., Yun, J., Shao, L. Carbon dioxide absorption with aqueous amine solutions promoted by piperazine and 1-methylpiperazine in a rotating zigzag bed. *Fuel* **2021**, *302*, 121165.
47. Lin. C., Chen, Y. Performance of a cross-flow rotating packed bed in removing carbon dioxide from gaseous streams by chemical absorption. *Int. J. Greenhouse Gas Control*. **2011**, *5*, 668-675.
48. Wu, T., Hung, Y., Chen, M., Tan, C. CO_2 capture from natural gas power plants by aqueous PZ/DETA in rotating packed bed. *Sep. Purif. Technol*. **2017**, *186*, 309-317.
49. Jiao, W., Yang, P., Qi, G., Liu, Y. Selective absorption of H_2S with high CO_2 concentration in mixture in a rotating packed bed. *Chem. Eng. Process.* **2018**, *129*, 142-147.
50. Joel, A. S., Wang, M., Ramshaw, C., Oko, E. Process analysis of intensified absorber for post-combustion CO_2 capture through modelling and simulation. *Int. J. Greenhouse Gas Control.* **2014**, *21*, 91-100.
51. Yang, Y., Xiang, Y., Chu, G., Zou, H. A noninvasive X-ray techniques for determination of liquid holdup in a rotating packed bed. *Chem. Eng. Sci.* **2015**, *138*, 244-255.

Highlights:

1. Rate-based simulation of CO_2 absorption by the blended amine solutions of PZ + MDEA in a rotating packed bed
2. Application of MATLAB linked to Aspen Plus for the modeling and the extraction of physical and transport properties
3. Presenting differential elements for the solving mass and energy balances
4. Application of the property package of E-NRTL and PC-SAFT for the prediction of vapor and liquid physical and transport properties
5. Low deviation between the simulated data and the experimental data

Author Statement:

Arash Esmaeili: Conceptualization, Simulation, Validation, Writing

Amin Tamuzi: Code writing, Methodology

Tohid N. Borhani: Simulation advice, Visualization

Yang Xiang: Investigation of correlations and equations

Lei Shao: Project administration, Supervision, Review & Editing

Declaration of interests

☒ The authors declare that they have no known competing financial interests or personal relationships that could have appeared to influence the work reported in this paper.

☐ The authors declare the following financial interests/personal relationships which may be considered as potential competing interests: